Miniaturised dual-band implantable antenna for wireless biotelemetry

Y. Cho and H. Yoo✉

A miniaturised implantable antenna with dual-band operation the Medical Implant Communications Service (MICS) (402–405 MHz) and Industrial, Scientific, and Medical (ISM) (2400.0–2483.5 MHz) bands is presented. The size of the proposed antenna is 31.5 mm^3 (8.75 mm × 7.2 mm × 0.5 mm) which is the smallest size compared to previous implantable antennas. A serpentine-shaped radiating patch and open-end slot placed on the ground plane are used for miniaturisation. The performance of the antenna was evaluated from measurements and is based on good agreement with simulations.

Introduction: Implantable medical applications have attracted a great deal of interest for obtaining real-time and stored physiological data. An implantable antenna is the important component for communicating wirelessly with equipment external to the human body. These antennas have many challenges to consider, such as variation of dielectric properties in human tissue, which affects antenna performance, and specific absorption rate (SAR) for safety. In particular, miniaturisation of the antenna should be accomplished since implantable devices have size restrictions. Therefore, various techniques and designs for a compact size in an antenna have been proposed [1–7]. Various frequency bands have been used for medical implantable devices. The Medical Implant Communications Service (MICS) (402–405 MHz) band is used globally for biomedical applications. Furthermore, the Industrial, Scientific, and Medical (ISM) (2400–2483.5 MHz) band is usually used to switch between sleep and wake modes to conserve the battery and extend the lifetime of the implanted device. In this Letter, a dual-band planar inverted-F antenna (PIFA) is proposed for skin tissue implantation. To increase bandwidth and miniaturisation, an open-end slot is used on the ground plane [1]. By using an open-end slot on the ground plane and a serpentine radiating patch configuration, significant size reduction can be achieved. With a compact size of only 31.5 mm^3 (8.75 mm × 7.2 mm × 0.5 mm), this is the smallest antenna, compared to other implantable dual-band antennas. The antenna was simulated at a 3 mm depth in homogeneous skin phantom and inside the scalp of a realistic human phantom because the intent is skin implantation for medical applications such as intracranial pressure (ICP) monitoring [2, 3]. To consider safety, specific absorption rate (SAR) values in the human phantom, and allowable input power were calculated.

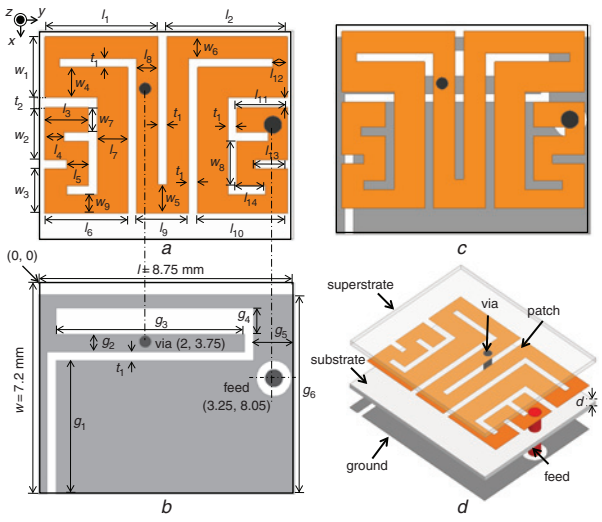

Fig. 1 *Geometry of proposed antenna*

a Radiating patch
b Ground
c Top view without substrate and superstrate
d Exploded view

Method: The geometry and dimensions of the proposed compact antenna are shown in Fig. 1, with dimensions of 8.75 mm × 7.2 mm × 0.5 mm (31.5 mm^3) which occupies the smallest volume compared to other antennas. A biocompatible dielectric material, Rogers 6010 ($\varepsilon_r = 10.2$, $\tan\delta = 0.0035$), is used as substrate as well as superstrate, with a thickness of 0.25 mm for each. As seen in Fig. 1*a*, the radiating patch has a serpentine structure. A coaxial feed with a 0.6 mm diameter and a shorting pin (via) with 0.4 mm diameter are located in different places. Moreover, the ground plane has a slot with one end open (Fig. 1*b*), and a significant miniaturisation effect can be observed. Figs. 1*c* and *d* show the top view without substrate and superstrate, and the exploded view, respectively. The detailed parameters of the antenna are listed in Table 1.

Table 1: Detailed dimensions of the proposed antenna (unit: millimetres)

Symbol	Value	Symbol	Value	Symbol	Value	Symbol	Value
l_1	3.9	l_9	1.8	w_3	1.55	g_1	4.55
l_2	4.15	l_{10}	3.1	w_4	1.05	g_2	0.6
l_3	1.5	l_{11}	1.75	w_5	1	g_3	6.45
l_4	0.65	l_{12}	0.5	w_6	0.75	g_4	0.9
l_5	0.75	l_{13}	1.1	w_7	0.85	g_5	1.4
l_6	2.85	l_{14}	1	w_8	1.55	g_6	3.7
l_7	1.05	w_1	2.1	w_9	0.65	t_1	0.3
l_8	0.75	w_2	1.8	d	0.25	t_2	0.35

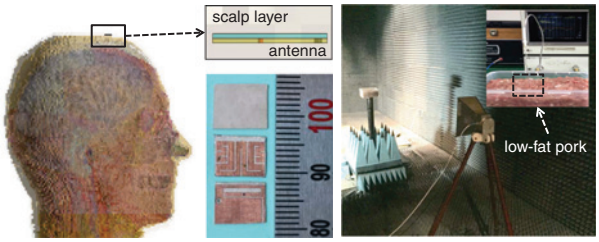

Fig. 2 *Simulation environment and measurement setup*

a Antenna implantation at a 3 mm depth inside head phantom; and fabricated antenna itself
b Measurement setup with low-fat pork

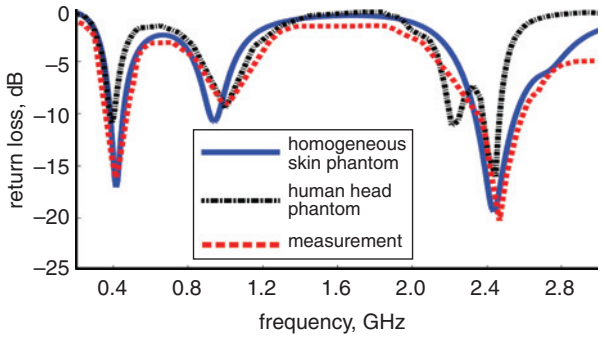

Fig. 3 *Comparison of $|S_{11}|$ for simulation setup of homogeneous skin phantom, human head phantom, and experimental measurement*

Fig. 2 illustrates the simulation (Fig. 2*a*) and measurement (Fig. 2*b*) setup. In simulations conducted with Sim4Life XFdtd simulation, the proposed antenna was initially placed at a 3 mm depth inside a homogenous skin phantom sized at 200 mm × 200 mm × 200 mm. This size for the human phantom was selected to represent the human head's volume. For further validation and to calculate the SAR, the antenna was implanted inside the scalp of a human head (DUKE model: male, 32 years old) because the intended application for the antenna is ICP monitoring on the human scalp. The dielectric properties of the phantoms are fully frequency-dependent as defined by Gabriel *et al.* [8].

Results and discussion: To validate the simulation results, the reflection coefficient (S_{11}) and the gain were measured. As shown in Fig. 2, the fabricated antenna was placed in a low-fat pork phantom (200 mm × 150 mm×100 mm) to maintain dielectric properties similar to human tissue. A comparison of $|S_{11}|$ between a homogeneous skin box, a human head, and the experimental measurements are shown in Fig. 3. As we can see from this figure, −10 dB bandwidth under the three different conditions cover the MICS band and the ISM band. To be more specific, the bandwidths ($|S_{11}|$ less than −10 dB) on the MICS band for the skin phantom, the head phantom, and the pork phantom

were 67 MHz (386–453 MHz), 28 MHz (379–407 MHz), and 91 MHz (371–462 MHz), respectively. On the ISM band, bandwidths for each setup were 246 MHz (2330–2577 MHz), 88 MHz (2377–2465 MHz), and 214 MHz (2376–2590 MHz). In the human head and the phantom, the resonance frequency shifted due to the heterogeneous tissue environment of the human body. Therefore, for recovery of frequency shifting or detuning, the length of the open-end ground slot and the position of the shorting pin can be varied. Comparison between the simulated gains for the homogeneous skin box and the human head, and the measured gain for the pork phantom, are shown in Fig. 4. Peak gains of −39.1 dBi at 402 MHz (Fig. 4*a*) and −21.2 dBi at 2450 MHz (Fig. 4*b*) were found for the human head phantom and the skin phantom, respectively. From the radiation patterns, we can see that the direction of maximum radiation at the two frequencies is in the Z+ direction, which is toward the exterior the body. In addition, the shape of the gain pattern for both the measurement and the human head phantom showed good agreement. For safety concerns, the standard SAR values under IEEE regulations are generally used. Table 2 shows the 1 and 10 g peak spatial-average SAR values of the proposed antenna at 402 and 2450 MHz, and the allowed transmitter power. When 1 W input power is delivered, the peak 1 g-average SAR values are 778.1 W/kg at 402 MHz and 491.9 W/kg at 2450 MHz. The peak 10 g-average SAR values are 87.4 W/kg at 402 MHz and 59.0 W/kg at 2450 MHz. These values mean the maximum output power to reach the safety level of 1.6 W/kg with 1 g SAR is between 2.1 and 3.3 mW, whereas for 10 g SAR with a safety level of 2 W/kg, maximum output power is between 22.9 and 33.9 mW. Comparison of the proposed antenna performance with previously reported implantable dual-band antennas is shown in Table 3. According to this table, the size of the proposed antenna has been significantly reduced, compared to other implantable antennas. Although the SAR values of the proposed antenna are bigger compared to the antenna of Xu *et al.* [7], this is acceptable. In addition, an acceptable bandwidth and good radiation performance are achieved in spite of the compact size.

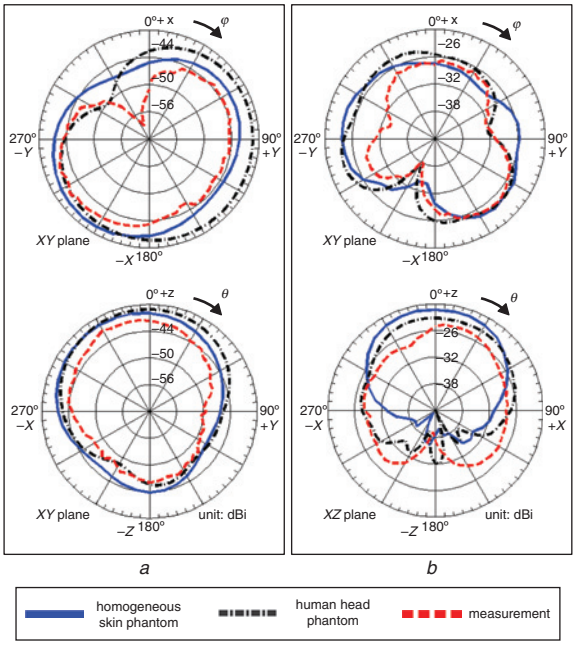

Fig. 4 *Azimuthal (XY-plane) and elevation (XZ-plane) far-field gain radiation patterns of proposed antenna at*

a 402 MHz
b 2450 MHz

Table 2: Peak spatial-average SAR (input power = 1 W) and maximum allowable net-input power for the proposed antenna

Frequency (MHz)	Max SAR (W/kg)		Max net-input power (mW)	
	1 g-avg	10 g-avg	1 g-SAR limit	10 g-SAR limit
402	778.1	87.4	2.1	22.9
2450	491.9	59.0	3.3	33.9

Table 3: Comparison of the proposed antenna with other antennas

Ref.	Dimensions (mm × mm × mm)	Bandwidth ($\|S_{11}\|$ < −10 dB)	Peak gain (dBi)	SAR (W/kg)	
				1 g-avg	10 g-avg
[3]	22.5 × 22.5 × 2.5 (1265.6 mm^3)	MICS: 35.3%	−24	–	
		ISM: 7.1%	−7.5		
[5]	16.5 × 16.5 × 2.54 (691.515 mm^3)	MICS: 13%	−31	318	–
		ISM: 4.4%	−9	292	–
[6]	13.4 × 16 × 0.835 (179.0 mm^3)	MICS: 16.5%	−30.6	–	85.2
		ISM: 24.7%	−19.1	–	77.8
[7]	10.02 × 10.02 × 0.675 (67.8 mm^3)	MICS: 47.5%	−30.5	302.4	40.3
		ISM: 31.6%	−19.2	238.9	39.2
This work	8.75 × 7.2 × 0.5 (31.5 mm^3)	MICS: 21.8%	−39.1	778.1	87.4
		ISM: 8.6%	−21.2	491.9	59.0

Conclusion: In this Letter, a miniature dual-band implantable antenna at 31.5 mm^3 (8.75 mm × 7.2 mm × 0.5 mm) was developed for biotelemetry applications. A large reduction in antenna size was achieved by inserting the shorting pin and the open-end slot on the ground plane. Simulation and experimental results showed good agreement as to satisfactory performance of the proposed implantable antenna despite the compact size and in comparison with previous implantable dual-band antennas.

Acknowledgment: This work was supported by the 2016 Research Fund of University of Ulsan.

Submitted: *5 April 2016* E-first: *12 May 2016*
doi: 10.1049/el.2016.1051
One or more of the Figures in this Letter are available in colour online.

Y. Cho and H. Yoo (*Department of Biomedical Engineering, School of Electrical Engineering, University of Ulsan, Ulsan, Republic of Korea*)

✉ E-mail: hsyoo@ulsan.ac.kr

References

1 Xu, L.J., Guo, Y.X., and Wu, W.: 'Dual-band implantable antenna with open-end slots on ground', *IEEE Antennas Wirel. Propag. Lett.*, 2012, **11**, pp. 1564–1567
2 Kiourti, A., and Nikita, K.S.: 'Miniature scalp-implantable antennas for telemetry in the MICS and ISM bands: design, safety considerations and link budget analysis', *IEEE Trans. Antennas Propag.*, 2012, **60**, (8), pp. 3568–3575
3 Karacolak, T., Hood, A.Z., and Topsakal, E.: 'Design of a dual-band implantable antenna and development of skin mimicking gels for continuous glucose monitoring'', *IEEE Trans. Microw. Theory Tech.*, 2008, **56**, (4), pp. 1001–1008
4 Lee, C.-M., Yo, T.-C., Huang, F.-J., and Luo, C.-H.: 'Dual-resonant Pi-shape with double L-strips PIFA for implantable biotelemetry', *Electron. Lett.*, 2008, **44**, pp. 837–838
5 Liu, C., Guo, Y.X., and Xiao, S.: 'Compact dual-band antenna for implantable devices', *IEEE Antennas Wirel. Propag. Lett.*, 2012, **11**, pp. 1508–1511
6 Duan, Z., Guo, Y.X., Je, M., and Kwong, D.L.: 'Design and in vitro test of a differentially fed dual-band implantable antenna operating at MICS and ISM bands', *IEEE Trans. Antennas Propag.*, 2014, **62**, pp. 2430–2439
7 Xu, L.J., Guo, Y.X., and Wu, W.: 'Miniaturized dual-band antenna for implantable wireless communications', *IEEE Antennas Wirel. Propag. Lett.*, 2014, **13**, pp. 1160–1163
8 Gabriel, C., Gabriel, S., and Corthout, E.: 'The dielectric properties of biological tissues', *Phys. Med. Biol.*, 1996, **41**, pp. 2231–2293